

1 **Duplication events downstream of *IRXI* cause North Carolina macular dystrophy at**
2 **the MCDR3 locus**

3

4 Valentina Cipriani,^{1,2,3,§,*} Raquel S Silva,^{1,2,§} Gavin Arno,^{1,2} Nikolas Pontikos,^{1,3} Ambreen
5 Kalhor,^{1,2} Sandra Valeina,⁴ Inna Inashkina,⁵ Mareta Audere,^{5,6} Katrina Rutka,^{5,6} Bernard
6 Puech,⁷ Michel Michaelides,^{1,2} Veronica van Heyningen,¹ Baiba Lace,^{5,8} Andrew R
7 Webster,^{1,2,*} Anthony T Moore^{1,2,9,*}

8

9 ¹UCL Institute of Ophthalmology, London, UK, ²Moorfields Eye Hospital, London, UK,
10 ³UCL Genetics Institute, London, UK, ⁴Children's Clinical University Hospital, Riga,
11 Latvia, ⁵Latvian Biomedical Research and Study Centre, Riga, Latvia, ⁶Riga Stradins
12 University, Riga, Latvia ⁷Exploration de la Vision et Neuro-Ophthalmologie, Centre
13 Hospitalier Universitaire, Lille, France ⁸Centre Hospitalier de l'Université Laval, Québec,
14 Canada, ⁹Ophthalmology Department, UCSF School of Medicine, San Francisco, CA,
15 USA

16

17 [§]These authors contributed equally to this work

18 ^{*}To whom correspondence should be addressed.

19

20 **Corresponding authors:** Valentina Cipriani, PhD, UCL Institute of Ophthalmology, 11-
21 43 Bath Street, London, EC1V 9EL, United Kingdom; email: v.cipriani@ucl.ac.uk;
22 phone: +44 (0)207 608 4042; fax: +44 (0)207 608 6830; Andrew R. Webster, MD (Res),
23 FRCOphth, UCL Institute of Ophthalmology, 11-43 Bath Street, London, EC1V 9EL,

24 United Kingdom; email: andrew.webster@ucl.ac.uk; Anthony T. Moore, MA,
25 FRCOphth, UCSF School of Medicine, Koret Vision Center, 10 Koret Way, San
26 Francisco, California (USA); email: tony.moore@ucsf.edu

27 **Abstract**

28 Word count: 192/200

29 Autosomal dominant North Carolina macular dystrophy (NCMD) is believed to represent
30 a failure of macular development. The disorder has been assigned by linkage to two loci,
31 MCDR1 on chromosome 6q16 and MCDR3 on chromosome 5p15-p13. Recently, non-
32 coding variants upstream of *PRDM13* and a large duplication including *IRX1* have been
33 identified. However, the underlying disease-causing mechanism remains uncertain.
34 Through a combination of sequencing studies, we report two novel overlapping
35 duplications at the MCDR3 locus, in a gene desert downstream of *IRX1* and upstream of
36 *ADAMTS16*. One duplication of 43 kb was identified in nine NCMD families (with
37 evidence for a shared ancestral haplotype), and another one of 45 kb was found in a
38 single family. The MCDR3 locus is thus refined to a shared region of 39 kb that contains
39 DNase hypersensitive sites active at a restricted time window during retinal
40 development. Publicly available data confirmed expression of *IRX1* and *ADAMTS16* in
41 human fetal retina, with *IRX1* preferentially expressed in fetal macula. These findings
42 represent a major advance in our understanding of the molecular genetics of NCMD at
43 the MCDR3 locus and provide insights into the genetic pathways involved in human
44 macular development.

45

46 **Abbreviations list**

47 aCGH – array comparative genomic hybridization

48 CNV – Copy number variant

49 IBD – Identical-by-descent

- 50 iPSC – Induced pluripotent stem cell
- 51 DHS – DNase hypersensitive site
- 52 HH – Homozygosity Haplotype
- 53 MCDR – Macular dystrophy region
- 54 NCMD – North Carolina macular dystrophy
- 55 PCR – Polymerase chain reaction
- 56 RCHH – Region with a Conserved Homozygosity Haplotype
- 57 SNP – Single-nucleotide polymorphism
- 58 SNV – Single nucleotide variant
- 59 SV – Structural variant
- 60 WGS – Whole-genome sequencing
- 61

62 **Introduction**

63

64 North Carolina macular dystrophy (NCMD) is a rare autosomal dominant disorder in
65 which there is abnormal development of the macula, a crucial structure of the central
66 retina responsible for central vision and colour perception¹. Understanding the genetics of
67 rare developmental macular conditions is key for unravelling the mechanism of
68 development of this structure that is found only in higher primates within mammals¹.
69 NCMD shows fully penetrant inheritance and is considered a non-progressive disorder
70 with a wide range of phenotypic manifestations, usually affecting both eyes
71 symmetrically^{2,3}. Phenotypic presentation varies from mild cases with drusen-like
72 deposits covering the macular region but with little or no visual impairment, to severe
73 cases with marked central chorioretinal atrophy and poor vision. Although generally non-
74 progressive, complications associated with choroidal neovascularization can contribute to
75 visual deterioration.

76 The molecular genetics of NCMD has been extensively investigated with the disorder
77 being mapped to chromosome 6q16 (MCDR1, MIM:136550) in multiple families of
78 different ethnic origins since the early 1990s⁴⁻¹⁰. A similar phenotype has been assigned
79 to a second locus at 5p15-13 (MCDR3, MIM:608850)^{11,3}. Interestingly, several studies
80 reported evidence for ancestral haplotypes at the MCDR1 locus^{2,12,13}. Early sequencing
81 studies of the two disease intervals failed to identify exonic disease-causing variants^{2,14}.
82 More recently, three novel single nucleotide variants (SNVs) were identified in 11
83 families at the MCDR1 locus, within a DNase1 hypersensitivity site (DHS), in the non-
84 coding interval between *PRDM13* and the neighbouring overlapping genes

85 *CCNC/TSTD3*¹⁵. Two tandem duplications including the full coding region of *PRDM13*,
86 with some additional upstream and downstream sequence included, were also
87 identified^{15,16}. One MCDR3-linked family of Danish origin³ was found to carry a 900 kb
88 tandem duplication¹⁵ that includes the entire coding sequence of *IRX1*. However,
89 duplications of *IRX1* have been observed in several normal individuals from the Database
90 of Genome Variants^{15,17} and the significance of this reported variant is uncertain. Thus,
91 the causative mechanism at the 5p15-13 NCMD locus remains unclear.

92 In this report we present a combination of genomic investigations in a cohort of 18
93 NCMD families. The aim of this study was to identify any causative molecular changes
94 and mechanism of disease in these families.

95

96 **Results**

97

98 *Families and brief clinical phenotype description*

99 Eighteen families with phenotypes consistent with a diagnosis of NCMD were included
100 in the study (Table 1 and Supplementary Fig. S1). Four families were previously
101 reported: suggestive linkage at the MCDR3 locus has been recently described for family
102 1¹⁴, family 2 was originally reported to be linked to the MCDR3 locus¹¹, and families 12
103 and 13 were linked to MCDR1^{7,9}, with family 13 recently found to carry the SNV V2
104 upstream of *PRDM13*¹⁵. All families (mostly of small size) showed autosomal dominant
105 inheritance and had at least one individual with Grade 3 disease. DNA samples from a
106 total of 56 affected and 33 unaffected family members were available for genetic
107 analysis.

108 Figure 1 shows fundus autofluorescence and optical coherence tomography (OCT)
109 images for selected individuals from families 2 and 3. Individual IV:5 from family 2
110 presents with a well demarcated, relatively symmetrical, bilateral area of macular
111 chorioretinal atrophy, while individual IV:3 from family 3 shows a mild form of disease
112 with relatively symmetrical, bilateral hyperfluorescent drusen-like deposits concentrated
113 in the macular region.

114

115 *Haplotype sharing analysis can exclude or suggest genetic mapping at known NCMD*
116 *loci*

117 Haplotype sharing analysis was carried out using the Homozygosity Haplotype (HH)
118 method¹⁸ to search for shared identical-by-descent (IBD) chromosomal segments among
119 affected individuals within each family. This analysis was performed in those families for
120 which Illumina single-nucleotide polymorphism (SNP) array data were available for
121 more than one affected family member (families 1-5 and 12-13). The 6q16 MCDR1 locus
122 was excluded in four families, including the two previously MCDR3-linked families 1¹⁴
123 and 2¹¹ and unreported families 3 and 4 (Supplementary Figs. S2-S5). Family 5 showed
124 evidence for haplotype sharing at many regions across the genome, including both the
125 6q16 and 5p15-p13 loci (Supplementary Fig. S6). The two previously reported MCDR1-
126 linked families 12⁷ and 13⁹ were confirmed with evidence for a Region with a Conserved
127 HH (RCHH) at the 6q16 locus, and not at the 5p15-p13 locus (Supplementary Figs. S7-
128 S8).

129

130 *Two additional NCMD families shown to carry previously reported SNV upstream of*

131 ***PRDM13 at the MCDR1 locus***

132 All families, except families 1-4 for which linkage at the 6q16 locus had been excluded
133 via haplotype sharing analysis, were tested with Sanger Sequencing for the three
134 previously reported SNVs (V1-V3) upstream of *PRDM13*¹⁵. In addition to the previously
135 reported V2 family 13¹⁵, two more NCMD families were found to harbour the variant V2
136 (family 11 and the previously described MCDR1-linked family 12⁷).

137

138 ***Array-based comparative genomic hybridization (aCGH) uncovers duplications at the***
139 ***MCDR3 locus in three NCMD families***

140 To investigate the MCDR3 locus for the presence of structural variants (SVs), an aCGH
141 experiment using 10,000 probes spanning the region at chr5:11882-10140073
142 (GRCh37/hg19) was performed in three affected individuals from families 1-3 which did
143 not show linkage at the 6q16 locus (Supplementary Figs. S2-S4). All three families were
144 found to harbour heterozygous duplications of approximately 45kb, downstream of *IRX1*
145 and upstream of *ADAMTS16* (Fig. 2a). The duplications were found to be located in the
146 minimal overlapping regions chr5:4391880-4434888 (GRCh37/hg19) in family 1 and
147 chr5:4397221-4440150 (GRCh37/hg19) in families 2 and 3. These SVs were not seen in
148 16 control individuals included in the same aCGH experiment, nor were they present in
149 WGS data from 650 individuals with inherited retinal disease¹⁹ or in publicly available
150 population data (CNV browser)²⁰.

151

152 ***WGS identifies four more NCMD families with duplications at the MCDR3 locus***

153 Thirteen affected individuals from families 1-7 underwent whole genome sequencing

154 (WGS). Graphical visualisation of individual paired-end reads using Integrative
155 Genomics Viewer (IGV)^{21,22} confirmed the presence of heterozygous tandem
156 duplications in families 1-3 (Fig. 2b). Precise breakpoint coordinates were identified from
157 coverage changes, split reads and chimeric reads. Family 1 had a 45158 bp duplicated
158 region (GRCh37/hg19 chr5:4391377-4436535) and families 2 and 3 shared an identical
159 43515 bp tandem duplication (GRCh37/hg19 chr5:4396927-4440442), overlapping the
160 first identified SV by 85% of the sequence (GRCh37/hg19 chr5:4396925-4436534).
161 Subsequently, members from families 4-7 were also found to carry the same 43 kb
162 duplication.
163 PCR primers were designed to amplify the novel sequence across the breakpoint between
164 duplicated copies (Table 2, Fig. 3) and used to confirm the predicted breakpoints and
165 assess segregation of the two variants in all available affected and unaffected members of
166 families 1 and 2 (Fig. 3, Table 1 and Supplementary Fig. S1). PCR was then used to
167 genotype the available affected individuals from families 3-7 and confirmed the presence
168 of a band in all affected individuals tested (Table 1 and Supplementary Fig. S1).

169

170 ***Genotyping reveals three additional previously unmapped NCMD families with***
171 ***duplications at the MCDR3 locus***

172 The remaining 8 unmapped families were tested with the established PCR assay for both
173 duplications, and 3 of them (families 8-10) were also found to carry the 43 kb duplication
174 (Table 1 and Supplementary Fig. S1). Thus, a total of 9 not knowingly related families
175 were shown to harbour the same 43 kb tandem duplication at the MCDR3 locus. Five

176 affected members available from the remaining 5 families did not carry either of the two
177 novel duplications.

178

179 ***Haplotype sharing analysis suggests presence of ancestral haplotypes at the MCDR1***
180 ***and MCDR3 loci***

181 We hypothesized that finding the same 6q16 SNV and 5p15 duplication with identical
182 breakpoint in 3 and 9 families respectively, could be due to two different shared ancestral
183 haplotypes suggestive of a common founder, in keeping with previous reports on other
184 6q16 NCMD families^{5,12,13,15}. Therefore, haplotype sharing analysis was performed using
185 available Illumina SNP array data from 14 affected individuals in 3 families carrying the
186 6q16 V2 variant (families 11-13) and 14 affected individuals in 6 families carrying the
187 5p15 43 kb duplication (families 2-7). Using a cut-off of 2.0 cM and 2.5 cM respectively,
188 the results confirmed that all the genotyped 6q16 individuals collectively shared a RCHH
189 of approximately 2.5 Mb from GRCh37/hg19 coordinate chr6:98962591 (rs150396) to
190 chr6:101468591 (rs1321204) at the MCDR1 locus, and all the genotyped 5p15
191 individuals collectively shared a RCHH of approximately 0.9 Mb from GRCh37/hg19
192 coordinate chr5:4327455 (rs155354) to chr5:5210050 (rs1560063) at the MCDR3 locus
193 (Supplementary Tabs. S1-S2 and Supplementary Figs. S9-S10).

194

195 **Discussion**

196

197 We report two distinct heterozygous tandem duplications at the MCDR3 locus in 30
198 affected individuals from 10 NCMD families. The two novel SVs overlap the previously
199 described duplication found in a single NCMD family of Danish origin¹⁵ and further
200 refine the 5p15 NCMD locus to a shared region of 39 kb in a gene desert downstream of
201 *IRX1* and upstream of *ADAMTS16* (800 kb and 693.9 kb from the respective transcription
202 start sites, Fig. 4).

203 We postulated that the 39 kb shared region could harbour *cis*-acting elements that
204 contribute to the fine tuning of gene expression during macular development, affecting
205 target gene expression spatially, temporally and/or quantitatively. Publicly available
206 platforms were queried for informative data on gene expression and chromatin
207 accessibility in relevant tissue types. A dataset screening for gene expression in fetal
208 retina confirmed high expression of *IRX1* at 19-20 weeks of gestation in the macula, and
209 medium expression levels in other regions (Supplementary Fig. S11). In contrast,
210 *ADAMTS16* had medium expression levels throughout the retina^{23,24}. Although no role in
211 retinal pathophysiology has been described for *ADAMTS16*, the gene has high sequence
212 similarity to *ADAMTS18* which has been previously associated with retinal disease³².
213 Overall, the data suggest that the pattern and/or refined spatial dosage and timing of
214 expression of the transcription factor *IRX1* may be important in macular development. A
215 second dataset provided information on open chromatin conformation using DNase-
216 accessible sequencing in fetal retina tissues at 5 stages from gestation day 72 to 125 (~10
217 to 18 weeks)²⁵. Different sites were identified to be open/active within the 39 kb shared

218 region at four out of five time points (~10-15 weeks of gestation) available during retinal
219 development (Table 3). Interestingly, one of the sites was active during three
220 developmental stages and the remaining four sites were functionally active as two
221 overlapping pairs. At the last time point (day 125, ~18 weeks), all sites were
222 inactive/closed. In the context of human macular development, the sites are active during
223 the period where photoreceptors are proliferating and differentiating²⁶; by week 14 of
224 gestation, cells of the central retina exit mitosis²⁶, corresponding to the period where
225 DHSs are turning off.

226 As mentioned, the MCDR1 locus on chromosome 6q16 is associated with variants sited
227 within a DHS, which suggests that aspects of macular development may be highly gene
228 dosage sensitive. Exploring the function and precise target of such regulatory domains in
229 both loci will be essential for understanding the disease mechanism of NCMD and
230 investigating its potential role in the context of normal macular development. The graded
231 expression of *IRX1* and known involvement in retinal development^{27,28}, but not
232 *ADAMTS16* in the macular region, suggests that *IRX1* is the probable target of the
233 putative retinal regulatory element which, when duplicated, may cause misregulation of
234 *IRX1*.

235 Eye development, like other organogenesis processes, requires the precise spatio-
236 temporal and quantitative expression of genes, orchestrated by a complex network of
237 regulatory mechanisms influencing critical transcription factors and other developmental
238 genes. The lack of readily accessible animal or *in vitro* models has hindered detailed
239 understanding of macular development, as this structure only evolved in higher primates
240 among mammals. Recently, disrupted developmental expression of the transcription

241 factor and histone methyltransferase *PRDM13*^{29,30} was suggested as a disease mechanism
242 for NCMD at the 6q16 locus, based on the identification of non-coding SNVs and
243 duplication events residing in an overlapping region upstream of *PRDM13* in many
244 MCDR1 families. Differential regulation of *PRDM13* in eyecups derived from wild-type
245 iPSCs^{15,16} was suggested. However, no causal relationship between the non-coding
246 variants and *PRDM13* expression has been identified.

247 Despite variable presentation in affected individuals, the NCMD phenotypic spectrum is
248 indistinguishable in patients assigned to either of the two linked loci, MCDR1 and
249 MCDR3. Whether a biological and functional connection between *PRDM13* at the
250 MCDR1 locus and the most likely candidate gene *IRX1* at the MCDR3 locus exists
251 warrants further investigation. iPSC technology and CRISPR manipulation in eye cups
252 from normal and affected individuals may help elucidate the molecular mechanism^{33,34}
253 and the potential molecular links between the two genes. Importantly, the involvement of
254 ancestral variation at both the 6q16 and 5p15 loci (Supplementary Figs. S9-S10) in such a
255 highly penetrant dominant disease is intriguing, with the implication that there may exist
256 a significant number of unrecognized related NCMD families. Full clinical examination
257 reveals a high degree of penetrance, but visually unaffected individuals in whole families
258 may fail to be ascertained.

259 Finally, the two novel duplications identified in this study significantly further the
260 understanding of the molecular genetics of NCMD at the MCDR3 locus and provide
261 additional effective tools for the molecular diagnosis of NCMD families.

262

263 **Materials and Methods**

264

265 *Families*

266 All families were ascertained at Moorfields Eye Hospital, London, United Kingdom,
267 expect for family 1¹⁴ (Vision Centre, Children's Clinical University Hospital, Riga,
268 Latvia) and family 13⁹ (Centre Hospitalier Régional Universitaire de Lille, France).
269 When possible, retinal imaging was undertaken using colour fundus photography, fundus
270 autofluorescence and OCT imaging. Blood/saliva samples were collected for DNA
271 extraction, genotyping and sequence analyses. The study protocol was approved by the
272 local ethics committees (Central Medical Ethics Committee of Latvian Republic; NRES
273 Committee London – Camden & Islington) and conformed to the tenets of the
274 Declaration of Helsinki. Written informed consent was obtained from all participants, or
275 their parents, before inclusion in the study.

276

277 *Genotyping*

278 Genomic DNA was extracted from whole blood/saliva and genotyped using the Illumina
279 HumanOmniExpress-24 v1.0 beadchip (Illumina, Inc., San Diego, CA, USA). Genotypes
280 were determined using the Genotyping Module in the Illumina GenomeStudio v2011.1
281 software.

282

283 *Haplotype sharing analysis*

284 In order to search for chromosomal segments sharing the same haplotype across affected
285 individuals (within the same family or across different families), the non-parametric HH
286 method¹⁸ was used for the analysis of those affected individuals that were genotyped with

287 the Illumina array. The HH is a type of haplotype described by the homozygous SNPs
288 only (all heterozygous SNPs are removed) and, therefore, can be uniquely determined on
289 each chromosome. Since affected family members who inherited the same mutation from
290 a common ancestor share a chromosomal segment IBD around the disease gene, they
291 should not have discordant homozygous calls in the IBD region and thus they should
292 share the same HH. The HH approach predicts IBD regions through the identification of
293 RCHHs defined as those regions with a shared HH among affected individuals and a
294 genetic length longer than a certain cut-off value (recommended cut-off for Illumina
295 HumanOmniExpress array is 2.5/3.0 cM for the analysis of one single family).

296

297 *aCGH*

298 aCGH was performed at Oxford Gene Technology (OGT) (Begbroke, United Kingdom)
299 using a custom design consisting of 10,000 probes spanning the MCDR3 locus at
300 GRCh37/hg19 chr5:11882-10140073 (approximately 1 probe every 1,000 bp), designed
301 with Agilent e-Array software (Agilent Technologies Inc., Santa Clara, CA, USA), in
302 three individuals from families 1-3 (Supplementary Fig. S1). Sixteen other individuals
303 affected by non-ocular phenotypes were also included in the experiment and used as
304 controls in the analysis. Scanned images of the arrays were processed with OGT
305 CytoSure™ Interpret Software v4.4 using the Accelerate Workflow for calling CNVs.
306 Duplications or deletions were considered when the \log_2 ratio of the Cy3/Cy5 intensities
307 of a region encompassing at least four probes was > 0.3 or < -0.6 , respectively (software
308 default settings).

309

310 ***WGS and bioinformatics analysis***

311 Whole-genome sequencing was performed using the Illumina HiSeq X10 platform
312 (Illumina, Inc., San Diego, CA, USA), generating minimum coverage of 30X. Reads
313 were aligned to the hg19 human reference sequence (build GRCh37) with novoalign
314 (version 3.02.08). The aligned reads were sorted by base pair position and duplicates
315 were marked using novosort. Discordant reads were marked with samblaster (version
316 0.1.20) and sent to a separate file for manual inspection of breakpoints using the IGV
317 (version 2.3.61). SVs were manually investigated using the IGV by identifying peaks of
318 discordant reads which were interpreted as breakpoints. The identified duplicated regions
319 were also screened for the presence of common copy number variants using data from the
320 CNV browser²⁰ (https://personal.broadinstitute.org/handsake/mcnv_data/) and WGS data
321 from 650 individuals with inherited retinal disease¹⁹.

322

323 ***Sanger sequencing validation of duplication events***

324 Segregation analysis of the duplication events identified by WGS was performed using
325 primers (Table 2) designed to span the end of first copy and start of second copy. A
326 graphical representation is shown in Fig. 3. After sequence confirmation with Sanger
327 sequencing, PCR was used to genotype selected individuals from all identified families.

328

329 ***In silico analysis of duplicated sequences and expression of flanking genes***

330 The Encyclopedia of DNA Elements (ENCODE)²⁵ was interrogated for fetal retina
331 datasets of interest. Bed files from DNA-seq datasets (ENCFF249FGP, ENCFF937NUZ,
332 ENCFF401BCF, ENCFF591NRB, ENCFF265ZNN, Stamatoyannopoulos' laboratory)

333 were downloaded and investigated at the shared duplicated region with R Studio. A
334 second microarray expression dataset on human fetal retina (19-20 gestation week) was
335 queried for the genes of interest²⁴ using the platform GENEVESTIGATOR²³.

336 References

- 337 1. Provis, J. M., Dubis, A. M., Maddess, T. & Carroll, J. Progress in Retinal and Eye
338 Research Adaptation of the central retina for high acuity vision: Cones, the
339 fovea and the avascular zone. *Prog. Retin. Eye Res.* **35**, 63–81 (2013).
- 340 2. Yang, Z. *et al.* Clinical characterization and genetic mapping of North Carolina
341 macular dystrophy. *Vision Research* **48**, 470–477 (2008).
- 342 3. Rosenberg, T. *et al.* Clinical and genetic characterization of a Danish family with
343 North Carolina macular dystrophy. *Mol. Vis.* **16**, 2659–2668 (2010).
- 344 4. Small, K. W. *et al.* North Carolina macular dystrophy is assigned to chromosome
345 6. *Genomics* **13**, 681–685 (1992).
- 346 5. Pauleikhoff, D. *et al.* Clinical and genetic evidence for autosomal dominant North
347 Carolina macular dystrophy in a German family. *American Journal of*
348 *Ophthalmology* **124**, 412–415 (1997).
- 349 6. Rabb, M. F., Mullen, L., Yelchits, S., Udar, N. & Small, K. W. A North Carolina
350 macular dystrophy phenotype in a Belizean family maps to the MCDR1 locus. *Am.*
351 *J. Ophthalmol.* **125**, 502–8 (1998).
- 352 7. Reichel, M. B. *et al.* Phenotype of a British North Carolina macular dystrophy
353 family linked to chromosome 6q. *Br. J. Ophthalmol.* **82**, 1162–1168 (1998).
- 354 8. Rohrschneider, K., Blankenagel, A., Kruse, F. E., Fendrich, T. & Völcker, H. E.
355 Macular function testing in a German pedigree with North Carolina macular
356 dystrophy. *Retina* **18**, 453–9 (1998).
- 357 9. Small, K. W., Puech, B., Mullen, L. & Yelchits, S. North Carolina macular
358 dystrophy phenotype in France maps to the MCDR1 locus. *Mol. Vis.* **3**, 1 (1997).
- 359 10. Small, K., Garcia, C., Gallardo, G., Udar, N. & Yelchits, S. North Carolina
360 macular dystrophy (MCDR1) in Texas. *Retina* **18**, 448–452 (1998).
- 361 11. Michaelides, M. *et al.* An early-onset autosomal dominant macular dystrophy
362 (MCDR3) resembling North Carolina macular dystrophy maps to chromosome 5.
363 *Investig. Ophthalmol. Vis. Sci.* **44**, 2178–2183 (2003).
- 364 12. Sauer, C. G. *et al.* An ancestral core haplotype defines the critical region
365 harbouring the North Carolina macular dystrophy gene (MCDR1). *J. Med. Genet.*
366 **34**, 961–966 (1997).
- 367 13. Small, K. W. North Carolina macular dystrophy: clinical features, genealogy, and
368 genetic linkage analysis. *Trans. Am. Ophthalmol. Soc.* **96**, 925–961 (1998).
- 369 14. Audere, M. *et al.* Genetic linkage studies of a North Carolina macular dystrophy
370 family. *Medicina (Kaunas)*. **52**, 180–186 (2016).
- 371 15. Small, K. W. *et al.* North Carolina Macular Dystrophy Is Caused by Dysregulation
372 of the Retinal Transcription Factor PRDM13. *Ophthalmology* **123**, 9–18 (2016).
- 373 16. Bowne, S. J. *et al.* North Carolina macular dystrophy (MCDR1) caused by a novel
374 tandem duplication of the PRDM13 gene. *Mol. Vis.* **22**, 1239–1247 (2016).
- 375 17. MacDonald, J. R., Ziman, R., Yuen, R. K. C., Feuk, L. & Scherer, S. W. The
376 Database of Genomic Variants: A curated collection of structural variation in the
377 human genome. *Nucleic Acids Res.* **42**, (2014).
- 378 18. Miyazawa, H. *et al.* Homozygosity haplotype allows a genomewide search for the
379 autosomal segments shared among patients. *Am. J. Hum. Genet.* **80**, 1090–102
380 (2007).

- 381 19. Carss, K. J. *et al.* Comprehensive Rare Variant Analysis via Whole-Genome
382 Sequencing to Determine the Molecular Pathology of Inherited Retinal Disease.
383 *Am. J. Hum. Genet.* **100**, 75–90 (2017).
- 384 20. Handsaker, R. E. *et al.* Large multiallelic copy number variations in humans. *Nat.*
385 *Genet.* **47**, 1–10 (2015).
- 386 21. Robinson, J. T. *et al.* Integrative genomics viewer. *Nat. Biotechnol.* **29**, 24–26
387 (2011).
- 388 22. Thorvaldsdóttir, H., Robinson, J. T. & Mesirov, J. P. Integrative Genomics Viewer
389 (IGV): High-performance genomics data visualization and exploration. *Brief.*
390 *Bioinform.* **14**, 178–192 (2013).
- 391 23. Hruz, T. *et al.* Genevestigator V3: A Reference Expression Database for the Meta-
392 Analysis of Transcriptomes. *Adv. Bioinformatics* **2008**, 1–5 (2008).
- 393 24. Kozulin, P. & Provis, J. M. Differential gene expression in the developing human
394 macula: Microarray analysis using rare tissue samples. *J. Ocul. Biol. Dis. Infor.* **2**,
395 176–189 (2009).
- 396 25. Dunham, I. *et al.* An integrated encyclopedia of DNA elements in the human
397 genome. *Nature* **489**, 57–74 (2012).
- 398 26. Provis, J. M., van Driel, D., Billson, F. A. & Russell, P. Development of the
399 human retina: patterns of cell distribution and redistribution in the ganglion cell
400 layer. *J. Comp. Neurol.* **233**, 429–51 (1985).
- 401 27. Choy, S. W. *et al.* A cascade of *irx1a* and *irx2a* controls *shh* expression during
402 retinogenesis. *Dev. Dyn.* **239**, 3204–3214 (2010).
- 403 28. Cheng, C. W., Yan, C. H. M., Hui, C. chung, Strähle, U. & Cheng, S. H. The
404 homeobox gene *irx1a* is required for the propagation of the neurogenic waves in
405 the zebrafish retina. *Mech. Dev.* **123**, 252–263 (2006).
- 406 29. Watanabe, S. *et al.* Prdm13 regulates subtype specification of retinal amacrine
407 interneurons and modulates visual sensitivity. *J. Neurosci.* **35**, 8004–20 (2015).
- 408 30. Hanotel, J. *et al.* The Prdm13 histone methyltransferase encoding gene is a Ptf1a-
409 Rbpj downstream target that suppresses glutamatergic and promotes GABAergic
410 neuronal fate in the dorsal neural tube. *Dev. Biol.* **386**, 340–357 (2014).
- 411 31. Cavodeassi, F., Modolell, J. & Gómez-Skarmeta, J. L. The Iroquois family of
412 genes: from body building to neural patterning. *Development* **128**, 2847–2855
413 (2001).
- 414 32. Chandra, A. *et al.* Expansion of ocular phenotypic features associated with
415 mutations in ADAMTS18. *JAMA Ophthalmol.* **132**, 996–1001 (2014).
- 416 33. Zhong, X. *et al.* Generation of three-dimensional retinal tissue with functional
417 photoreceptors from human iPSCs. *Nat. Commun.* **5**, 4047 (2014).
- 418 34. Schwarz, N. *et al.* Translational read-through of the RP2 Arg120stop mutation in
419 patient iPSC-derived retinal pigment epithelium cells. *Hum. Mol. Genet.* **24**, 972–
420 86 (2015).
- 421

422 **Figure legends**

423

424 **Figure 1 NCMD typical clinical presentation in two selected individuals from family**
425 **3 (IV:5) and family 2 (IV:5).** Each panel shows fundus autofluorescence and optical
426 coherence tomography (OCT) images. Individual IV:5 (a,b) from family 3 shows a mild
427 form of disease with relatively symmetrical, bilateral hyperfluorescent drusen-like
428 deposits concentrated within the macular region and an otherwise normal OCT.
429 Individual IV:3 (c,d) from family 2 presents with a well demarcated, relatively
430 symmetrical and bilateral area of macular chorioretinal atrophy.

431

432 **Figure 2 NCMD is caused by intergenic duplication events located between *IRX1***
433 **and *ADAMTS16*.** (a) aCGH experiment (10,000 probes spanning the MCDR3 locus at
434 GRCh37/hg19 chr5:11882-10140073, panel I) performed in three affected individuals
435 from families 1-3 that were found to harbour heterozygous duplications of approximately
436 43 kb (panel II) located in a gene desert downstream of *IRX1* and upstream of
437 *ADAMTS16* (panel III), also confirmed by WGS (b) by changes in coverage from
438 concordant and discordant reads (panel I and II, respectively) and identification of
439 chimeric reads, pair-reads with opposing orientation (displayed in green, panel III).
440 Panels are presented with a split view option within IGV. The duplications are located in
441 the overlapping regions GRCh37/hg19 chr5:4391880-4434888 (family 1) and
442 GRCh37/hg19 chr5:4397221-4440150 (families 2 and 3).

443

444 **Figure 3 PCR and Sanger sequencing validation of duplication breakpoints and**
445 **segregation in family 1 (a) and family 2 (b).** All available individuals (Supplementary
446 Fig. S1) were tested with primers designed across the predicted breakpoints to generate a
447 unique junction fragment sequence. The exact breakpoint is marked with a red bar; PCR
448 primers are represented with blue arrows. L = ladder; W = water; “-“ = genomic DNA
449 pooled from control individuals.

450

451 **Figure 4 Schematic representation of the MCDR3 locus which is refined to a 39 kb**
452 **shared genomic region (GRCh37/hg19 chr5:4396925-4436534).** The shared sequence
453 between a previously reported duplication and the two novel SVs identified in this study
454 is located in a large gene desert, downstream of *IRX1* and upstream of *ADAMTS16*, 800
455 kb and 693.9 kb from their respective transcription start sites. Publicly available NGS
456 datasets were queried for informative data on chromatin accessibility and 3 sites were
457 found active from human gestation day 72 to 105 in fetal retina, suggestive of functional
458 acting elements within this site.

459

460 **Acknowledgements**

461 The authors would like to acknowledge the ENCODE Consortium and
462 Stamatoyannopoulos' laboratory for generating the DNA-seq datasets queried in this
463 study, the NIHR BioResource - Rare Disease Consortium (Dr. Keren J Carss and Prof. F
464 Lucy Raymond) for access to CNV data from WGS data, Dr. Gabriela E Jones
465 (University Hospitals of Leicester NHS Trust, Leicester, UK) for help with patient
466 recruitment, Dr. V. Plagnol (UCL Genetics Institute, London, UK) for access to control

467 aCGH data, and UCL Computer Science Cluster and Technical Support (London, UK).
468 This work was supported by grants from the NIHR Biomedical Research Centre at
469 Moorfields Eye Hospital National Health Service Foundation Trust and UCL Institute of
470 Ophthalmology (London, UK), the Research to Prevent Blindness (USA), the British Eye
471 Research Foundation (UK), Fight for Sight (UK), the Macular Society (UK), Moorfields
472 Eye Hospital Special Trustees (UK), Moorfields Eye Charity (UK), the Foundation
473 Fighting Blindness (USA) and Retinitis Pigmentosa Fighting Blindness (UK). RSS is
474 funded through a Fight for Sight PhD studentship granted to ARW and VvH. The views
475 expressed in this publication are those of the authors and not necessarily those of the
476 funding bodies.

477

478 **Author Contributions Statement**

479 Study conception and design: ATM, ARW, VvH, VC, RSS, GA.

480 Patient recruitment and phenotyping: ATM, ARW, AK, MM, BP, BL, SV.

481 Acquisition of data: VC, RSS, GA, II, MA, KR.

482 Analysis and/or interpretation of data: VC, RSS, NP, GA.

483 Drafting of manuscript: VC, RSS.

484 Critical revision for important intellectual content: ATM, ARW, VvH, GA.

485 All authors have read and accepted the final version of the manuscript.

486

487 **Additional Information**

488 **Competing financial interests**

489 The authors declare no competing financial interests.

Tables

Table 1 Summary of families with two newly reported tandem duplications at the MCDR3 locus and previously identified V2 variant at the MCDR1 locus.

Family number	Family ID	Origin	Phenotype	Experimental procedure	Causative allele change	Nucleotide change	Number of affected family members analysed	Number of unaffected family members analysed	Total number of family members analysed
1	GC19806 ¹⁴	Latvian	NCMD	SNP, aCGH, WGS, PCR/Sanger	chr5:4391377-4436535	45158 bp duplication	5	1	
2	GC15626 ¹¹	British	NCMD	SNP, aCGH, WGS, PCR/Sanger	chr5:4396927-4440442	43515 bp duplication	9	8	
3	GC15119	British	NCMD	SNP, aCGH, WGS, PCR/Sanger	chr5:4396927-4440442	43515 bp duplication	4	0	
4	GC13840	British	NCMD	SNP, WGS, PCR/Sanger	chr5:4396927-4440442	43515 bp duplication	3	0	
5	GC19075	British	NCMD	SNP, WGS, PCR/Sanger	chr5:4396927-4440442	43515 bp duplication	3	0	
6	GC15475	British	NCMD	SNP, WGS, PCR/Sanger	chr5:4396927-4440442	43515 bp duplication	1	0	
7	GC11709	British	NCMD	SNP, WGS, PCR/Sanger	chr5:4396927-4440442	43515 bp duplication	1	0	
8	GC16913	British	NCMD	PCR/Sanger	chr5:4396927-4440442	43515 bp duplication	1	0	
9	GC4092	British	NCMD	PCR/Sanger	chr5:4396927-4440442	43515 bp duplication	1	0	
10	GC23501	British	NCMD	PCR/Sanger	chr5:4396927-4440442	43515 bp duplication	2	1	
11	GC15416	British	NCMD	SNP, PCR/Sanger	chr6:100040987	G>C (V2)	2	0	
12	GC3722 ⁷	British	NCMD	SNP, PCR/Sanger	chr6:100040987	G>C (V2)	12	8	
13	GC17225 ^{9,15}	French	NCMD	SNP, PCR/Sanger	chr6:100040987	G>C (V2)	12	15	
						Total	56	33	

Genomic coordinates refer to GRCh37/hg19 assembly. SNP, aCGH, WGS, PCR/Sanger indicate Illumina SNP array, array-based comparative genomic hybridization, whole-genome sequencing and Sanger Sequencing, respectively. Five affected members from five additional NCMD families were also tested for the presence of previously reported SNVs V1-V3¹⁵ and the two tandem duplications found in this study, but none of these affected individuals was found to carry any of the variants.

Table 2 Primer sequences used for the segregation analysis of the two novel MCDR3 duplications identified in the study.

Duplication size	Primer sequence		Tm (°C)	Length (bp)
43 kb	F	5' - TTGTGGACTGAGCAAGCAAG - 3'	63	532
	R	5' - GGAGCAGAAGTTAAATGTGGAGA - 3'		
45 kb	F	5' - TTTGCTTGATCAATTCTGCTG - 3'	63	500
	R	5' - TTCTCAGTTGGAAGAGCACAAA - 3'		

Tm=Temperature of melting.

Table 3 DHSs active during fetal retina development at the 39 kb shared duplicated region (GRCh37/hg19 chr5:4396925-4436534).

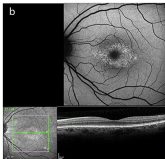
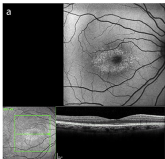
Chromosome	Start position	End position	Gestation day (fetal retina)
5	4418340	4418490	74
5	4420820	4420970	74, 89, 103
5	4418320	4418470	85
5	4420860	4421010	85
5	4409260	4409410	103

Gestation day 125 shows no active site at the 39 kb shared region. The fetal retina datasets were available from ENCODE²⁵, produced by the Stamatoyannopoulos' laboratory.

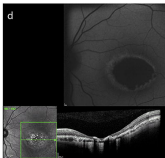
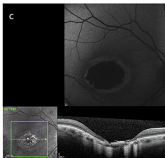
Right eye (OD)

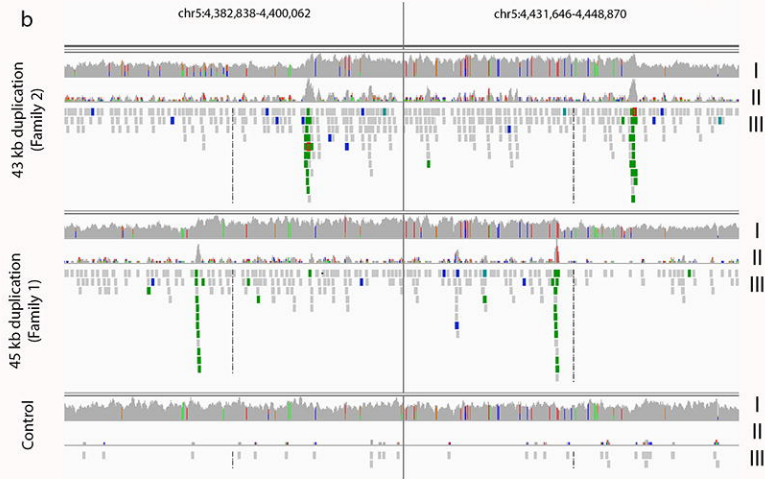
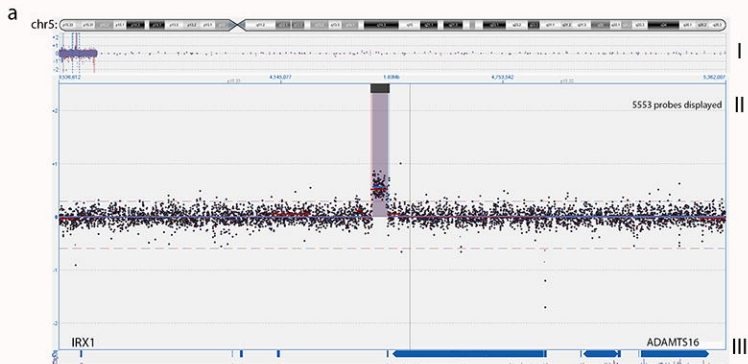
Left eye (OS)

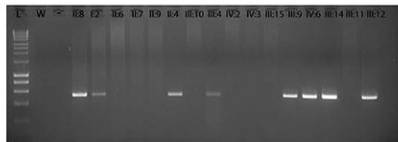
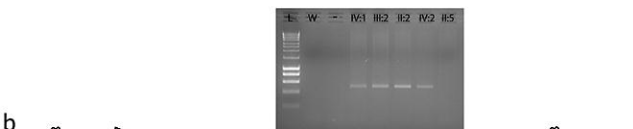
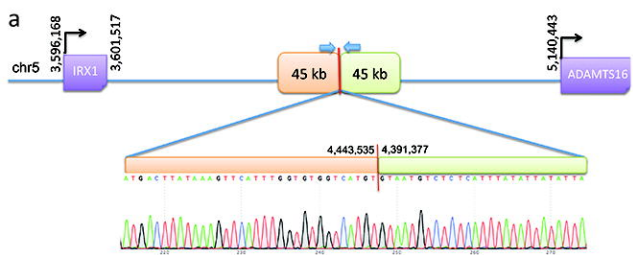
Family 3: IV:3



Family 2: IV:5







Coding
gene

lncRNA
RP11-44503

Predicted
enhancers

Predicted
insulators

Tandem
duplication

★ DHS active in fetal retina

